Geosci. Model Dev. Discuss., https://doi.org/10.5194/gmd-2018-253
Manuscript under review for journal Geosci. Model Dev.
Discussion started: 29 November 2018
© Author(s) 2018. CC BY 4.0 License.

Geoscientific Model Development Discussions

A parallel workflow implementation for PEST version 13.6 in high-performance computing for WRF-Hydro version 5.0: a case study over the Midwestern United States

Jiali Wang, Cheng Wang, Andrew Orr, Rao Kotamarthi

Argonne National Laboratory, Environmental Science Division, 9700 South Cass Avenue, Argonne, IL 60439, USA

Correspondence to: Jiali Wang (jialiwang@anl.gov)

Abstract. Surface hydrological models must be calibrated for each application region. The Weather Research and Forecasting Hydrological system (WRF-Hydro) is a state-of-the-art numerical model that models the entire hydrological cycle based on physical principles. However, as with other hydrological models, WRF-Hydro parameterizes many physical processes. As a result, WRF-Hydro needs to be calibrated to optimize its output with respect to observations. However, when applied to a relatively large domain, both WRF-Hydro simulations and calibrations require intensive computing resources and are best performed in parallel. Typically, each physics parameterization requires a calibration process that works specifically with that model, and is not transferrable to a different process or model. Parameter Estimate Tool (PEST) is a flexible and generic calibration tool that can calibrate any numerical code. However, PEST in its current configuration is not designed to work on the current generation of massively parallel high-performance computing (HPC) clusters. This study ported the parallel PEST to HPCs and adapted it to work with the WRF-Hydro. The porting involved writing scripts to modify the workflow for different workload managers and job schedulers, as well as developing code to connect Parallel-PEST to WRF-Hydro. We developed a case study using a flood in the Midwestern United States in 2013 to test the operational feasibility of the HPC-enabled parallel PEST. We then evaluate the WRF-Hydro performance in water volume and timing of the flood event. We also assess the spatial transferability of the calibrated parameters for the study area. We finally discuss the scale-up capability of the HPC-enabled parallel PEST to provide insight for PEST's application to other hydrological models and earth system models on current and emerging HPC platforms. We find that, for this particular study, the HPC-enabled PEST calibration tool can speed up WRF-Hydro calibration by a factor of 30 compared to commonly-used sequential calibration approaches.

Geosci. Model Dev. Discuss., https://doi.org/10.5194/gmd-2018-253
Manuscript under review for journal Geosci. Model Dev.
Discussion started: 29 November 2018
© Author(s) 2018. CC BY 4.0 License.

Geoscientific Model Development Discussions

1 Introduction

Hydrological models are important tools for research relevant but not limited to, water resource management, flood control, and hydrological response to climate change (Zanon et al., 2010; Papathanasiou et al., 2015). Conceptual hydrological models express hydrological processes in the form of abstract models that come from physical phenomenon and experience. Physically based hydrological models contain definite physical mechanisms to model the hydrological cycle, but many complex physical processes in these models are parameterized. For example, the state-of-the-art Weather Research and Forecasting Hydrological modeling system (WRF-Hydro; Gochis et al., 2015) has dozens of parameters that can be land- and river-type dependent and are typically specified in lookup tables. Both conceptual hydrological models and physically based hydrological models need to be calibrated before they can be applied to research. In this context, calibration refers to the hydrologists' need to adjust the values of the model parameters so that the model can closely match the behavior of the real system it represents. In some cases, the appropriate value for a model parameter can be determined through direct measurements conducted on the real system. However, in many situations the model parameters are conceptual representations of abstract watershed characteristics and must be determined through calibration. In fact, model calibration is the most time-consuming step, not only for hydrological models but also for earth system model development, because both parametric estimation and parametric uncertainty analysis require hundreds—if not thousands—of model simulations to understand how perturbations in model parameters affect simulations of dominant physical processes and to find the optimum value of a single parameter.

WRF-Hydro is a practical physics-based numerical model that can simulate the entire hydrological cycle using advanced high-resolution data such as satellite and radar products. Compared to the traditional land surface model (LSM) used by WRF, WRF-Hydro provides a framework for multiscale representation of surface flow, subsurface flow, channel routing, baseflow, as well as a simple lake/reservoir routing scheme. As a physics-based model, WRF-Hydro includes many complicated physical processes that are nonlinear and must be parameterized. For example, the parameters for channel routing are prescribed as functions of stream order, not space; thus the default parameters given by WRF-Hydro are only valid over a small region. Because channel routing can affect the accuracy of the model performance, calibration of related model parameters

© Author(s) 2018. CC BY 4.0 License.

is often required in order to use the model in a new domain. In particular, for a large spatial domain such as the entire Contiguous United States (CONUS), in order to develop the optimal parameter sets in a reasonable amount of time, the calibration must be conducted on HPCs in parallel instead of in the traditional sequential mode. To date, there is no such calibration tool that can straightforwardly calibrate WRF-Hydro on HPCs. Typically, each physics-based model needs a calibration code that is custom-designed to work with that particular numerical model. These custom-designed calibration codes/tools are highly challenging and do not offer flexibility; they are designed to operate with that particular numerical model and its set of physics parameterizations, software architecture, and solvers. Therefore, there is a need for a more flexible and generic calibration tool that can calibrate any code that uses Message Passing Interface/Open Multi Processing (MPI/OpenMP) for parallelization on HPCs.

There are two general types of calibration methods for hydrological models: manual calibration and automatic calibration. Models for individual catchments have traditionally been calibrated by manually adjusting key model parameters within established ranges of parameters to obtain a best match between observed and simulated discharges. This procedure is time consuming, dependent on the skill and experience of the modeler, and therefore prone to inconsistency between modelers. Automatic calibration is based on stochastic or mathematical methods and thus is more widely applicable for optimizing nonlinear parameters. Compared with manual calibration, automatic calibration is more efficient and effective, because it avoids interference from human factors (Madsen, 2000; Getirana, 2010). One widely used automatic calibration tool is Parameter Estimation Tool (PEST; Doherty 2016), which uniquely operates independent of models. There is no need to develop additional programs/codes for a particular model except preparing the files required by PEST as described in Sect. 3.2, because PEST works with that model through the model's own input and output files. PEST implements a particularly robust variant of the Gauss-Marquardt-Levenberg method (Levenberg, 1944; Marquardt, 1963) to estimate parameters. This method requires a continuous relationship to exist between model parameters and model outputs, but it can normally find the minimum in the objective function in a fairly shorter time period than other parameter estimation methods. This is especially important when model runs are lengthy or when many parameters must be calibrated. Parallel PEST is able to distribute many runs across many computing nodes using master-slave parallel programing. However, to the best of our

Geosci. Model Dev. Discuss., https://doi.org/10.5194/gmd-2018-253
Manuscript under review for journal Geosci. Model Dev.
Discussion started: 29 November 2018
© Author(s) 2018. CC BY 4.0 License.

knowledge, no approach is available that allows users to submit jobs using PEST parallelization to a typical supercomputing facility that uses job scheduling and workload management using Simple Linux Utility for Resource Management (SLURM), Portable Batch System (PBS), and Cobalt. A previous study (Senatore et al., 2015) used PEST to calibrate WRF-Hydro over the Crati River Basin in Southern Italy. However, because the study area was relatively small, they were able to conduct the calibration using PEST in sequential mode.

In this study, we ported parallel PEST to HPC clusters operated by the U.S. Department of Energy (DOE) and adapted it to work with WRF-Hydro. Porting involved writing additional scripts to modify the workflow for SLURM, Cobalt, and PBS and developing code to connect parallel PEST to WRF-Hydro. In particular, we aim to (1) calibrate the parameters of WRF-Hydro to improve model performance with realistic values maintaining their physical meanings; (2) speed up calibration for this particular study case and provide the capability to WRF-Hydro users; and (3) explore the scale-up capability of HPC-enabled parallel PEST linked to WRF-Hydro.

2 Model description

2.1 Study area

The case presented here is one of the worst floods experienced by greater Chicago area in the last three decades, which occurred on April 18, 2013 (Campos and Wang, 2015). According to the National Weather Service (NWS), the heaviest 24-hour accumulated rainfall during this storm reached 201.4, 171.1, and 136.4 mm across Illinois, Iowa, and Missouri, respectively. The Mississippi River crested at 10.8 m (1.7 m above flood stage), and the Illinois River crested in Peoria, Illinois, at 8.95 m; this broke the previous record of 8.78 m, set in 1943, and was 4.55 m above the historical normal river stage (NWS, 2013). Campos and Wang (2015) conducted three-domain nested WRF simulations to understand the dynamical and microphysical mechanisms of the event. Our study builds on the smallest domain of that study, which covers the majority of Illinois, Iowa, and Missouri at a spatial resolution of 3 km for the atmospheric and land surface model (Fig. 1).

Geosci. Model Dev. Discuss., https://doi.org/10.5194/gmd-2018-253
Manuscript under review for journal Geosci. Model Dev.
Discussion started: 29 November 2018
© Author(s) 2018. CC BY 4.0 License.

During the 10-day period of this studied case, light to moderate rain occurred on April 8 through 11, 2013, followed by a relatively dry period from April 12 to 14. Then a heavy rain event began on April 15 and peaked on April 18. The heaviest rain band moved east of the study area on April 19. The rainy event ended over the study area on April 20.

2.2 WRF-Hydro configuration

WRF-Hydro employs a multiscale modeling approach to handle the local landscape gradient features. Specifically, WRF-Hydro uses a subgrid disaggregation-aggregation procedure. For each time-step at which forcing data are available, the column moisture stays within the LSM and is disaggregated from the LSM grid to a high-resolution routing grid (Gochis and Chen 2003). After disaggregation, the routing schemes are executed using the high-resolution grid values. After execution of the routing schemes, the high-resolution grid values are aggregated back to the native LSM grid. For details of each routing component, see Gochis et al. (2015), Yucel et al. (2015), and Senatore et al. (2015).

Currently, two LSMs are available in WRF-Hydro for representing land-surface column physics: Noah (Chen and Dudhia, 2001) and Noah Multi-parameterization (NoahMP; Niu et al. 2011). We utilize NoahMP LSM because compared to Noah LSM it shows obvious improvements in reproducing surface fluxes, skin temperature over dry periods, snow water equivalent, snow depth, and runoff (Niu et al. 2011). Compared to LSM, one major advantage of WRF-Hydro system is that, WRF-Hydro system can keep the infiltration capacity exceedance as ponded water within the model domain. This ponded water is subsequently available for lateral redistribution, which combine the ponded water with new precipitation for calculating the infiltration amount in the next time step. WRF-Hydro has been tested in several different cases that focused on different hydrometeorological forecasting and simulation problems (e.g., Gochis et al., 2015; Yucel et al., 2015; Senatore et al., 2015; Arnault et al., 2016), and it shows reasonable accuracy in simulated streamflow.

This study employs WRF-Hydro version 5 with a basic configuration. This configuration does not use nudging technique as used in the National Water Model configuration and spatially distributed soil-related parameters. The LSM is at a grid spacing of 3 km and the aggregation factor is 15, that

Geosci. Model Dev. Discuss., https://doi.org/10.5194/gmd-2018-253
Manuscript under review for journal Geosci. Model Dev.
Discussion started: 29 November 2018
© Author(s) 2018. CC BY 4.0 License.

is, starting from a 3-km LSM resolution in the domain shown in Fig. 1, hydrological routing is performed at a spatial resolution of 200 m. We use a time step of 10 seconds for the routing grid to maintain model stability and prevent numerical dispersion of overland flood waves. The time step also meets the Courant condition criteria for diffusive wave routing on a 200-m resolution grid. The WRF-Hydro is configured to be offline or uncoupled mode — there is no online interaction with WRF atmospheric model. Surface flow, saturated subsurface flow, gridded channel routing, and a conceptual baseflow are active in this study. The gridded channel network uses an explicit, one-dimensional, variable time-stepping diffusive wave. A direct output-equals-input "pass-through" relationship is adopted here to estimate the baseflow. Although the baseflow module is not physically explicit, it is very important because the water flow in the channel routing are contributed by both overland flow and baseflow. If overland flow is active, it passes water directly to the channel model. In this case the soil drainage is the only water resource flowing into the baseflow buckets. If overland flow is deactivated but channel routing is still active, then WRF-Hydro collects excess surface infiltration water from the land model, and passes this water into the baseflow bucket. This bucket then contributes the water from both overland and soil drainage to the channel flow. Therefore, the baseflow must be active if the overland flow is switched off. This study does not consider lakes and reservoirs.

We use the geographic information system (GIS) tool that are developed by the WRF-Hydro team to delineate the stream channel network, open water (i.e., lake, reservoir, and ocean) grid cells, and groundwater/baseflow basins. Meteorological input for WRF-Hydro model system includes hourly precipitation; near-surface air temperature, humidity, wind speed; incoming shortwave and longwave radiation; and surface pressure. In this study, the hourly precipitation is from the National Centers for Environmental Prediction (NCEP) Stage IV analysis at a spatial resolution of 4 km. The Stage IV data is based on combined radar and gauge data (Lin and Mitchell, 2005; Prat and Nelson, 2015), and has been shown to be temporally well correlated with high-quality measurements from individual gauges (see, e.g., Sapiano and Arkin, 2009; Prat and Nelson, 2015). The other hourly meteorological input are from the second phase of the multi-institution North American Land Data Assimilation System project, phase 2 (NLDAS-2) (Xia et al., 2012a,b), at a spatial resolution of 12 km. NLDAS-2 is an offline data assimilation system featuring uncoupled LSMs that are driven by observation-based atmospheric forcing.

Geosci. Model Dev. Discuss., https://doi.org/10.5194/gmd-2018-253
Manuscript under review for journal Geosci. Model Dev.
Discussion started: 29 November 2018
© Author(s) 2018. CC BY 4.0 License.

3 Calibration

3.1 Platforms

We customized parallel PEST to work on two different workload managers and job schedulers: SLURM at the National Energy Research Scientific Computing Center (NERSC), PBS at Argonne National Laboratory Computing Resource Center, and Cobalt at Argonne Leadership Computing Facility. The tests presented here are conducted on Edison of NERSC, which uses the SLURM workload manager and job scheduler. Edison is a Cray XC30 with a peak performance of 2.57 petaflops per second, 133,824 compute cores, 357 terabytes of memory, and 7.56 petabytes of disk storage. It has 5,586 nodes and 24 cores per node.

3.2 PEST files

Parallel PEST requires four types of input file:

1. Template files, which define the parameters to be calibrated. For example, we generated CHANNEL.TPL, HYDRO.TPL, and GENPARAM.TPL based on the format of their corresponding lookup tables, which are CHANNEL.TBL, HYDRO.TBL, and GENPARAM.TBL, respectively. CHANNEL.TBL describes the features of a channel, such as bottom width, channel side slope, and Manning's roughness coefficients. HYDRO.TBL contains Manning's roughness coefficients for land-use types. GENPARAM.TPL describes the parameters used in the Noah-MP LSM.
2. An instruction file, which defines the format of model-generated output files. For example, WRF-Hydro can output time series of streamflow over the forecast points (frxst_pts_out.txt) specified during model configuration. The instruction file follows the format of frxst_pts_out.txt and specifies the line number of each calibrated forecast point in frxst_pts_out.txt.
3. A control file, which supplies PEST with the size of the problem (e.g., how many parameters to be calibrated; how many observational points); initial parameter values and their lower and upper bounds; the increment of each parameter for forward-calculation; the names of all template and instruction files; observational values, and weight for each parameter to be calibrated. PEST requires all these three file types in both sequential and parallel mode.

Geosci. Model Dev. Discuss., https://doi.org/10.5194/gmd-2018-253
Manuscript under review for journal Geosci. Model Dev.
Discussion started: 29 November 2018
© Author(s) 2018. CC BY 4.0 License.

4. To run PEST in parallel mode, one also needs a management file to inform PEST where each slave's working folder is, as well as the names and paths of each model input file PEST must write (i.e., lookup tables that come from template files) and each model output file PEST must read (such as frsxt_pts_out.txt).

Parallel PEST uses a "master-slave" paradigm that starts model runs simultaneously in different folders (or by different "slaves"). The master of parallel PEST communicates with each of its slaves many times during the course of a calibration. When PEST needs to run a model in a particular folder, the master notifies the slave to start the model in that folder. Each slave starts the model execution accordingly, and informs the master that the model starts running. Once the simulation is completed in a particular folder, the slave signals the master, so the mater can read the particular output However, to the best of our knowledge, parallel PEST is not designed to run on HPCs directly. We developed scripts and an interface to enable parallel PEST to run on HPCs using SLURM, PBS, or Cobalt workload managers and job schedulers. This enables parallel PEST to run many slaves on the HPC; each slave runs a parallel code (such as WRF-Hydro) that uses more than one node, which could significantly increase the computational performance of model calibrations. Although this master-slave parallelism may not be as efficient as a fully MPI approach, it is sufficient for model calibration and requires the least effort for the current parallel PEST to run on HPCs.

3.3 Calibrated experiments

The primary objective of this study is to present the operational and the scale-up capability of the HPC-enabled parallel PEST for use with WRF-Hydro calibration over a relatively large domain. We focus less on extensively assessing the performance of the WRF-Hydro model. The calibration and validation is limited to only 7 days, considering it is long enough to achieve our objective and to understand WRF-Hydro's sensitivity to multiple parameters. The calibration compares WRF-Hydro modeled river discharge to U.S. Geological Survey (USGS) surface water observations. We originally choose 11 USGS sites across the study area. However, because of inaccuracies introduced when projecting geospatial data from one coordinate system to another by the ArcGIS tool, three of the observational sites were not properly assigned to the desired location on the channel network. This situation is common in hydrographic data processing and well known to

Geosci. Model Dev. Discuss., https://doi.org/10.5194/gmd-2018-253
Manuscript under review for journal Geosci. Model Dev.
Discussion started: 29 November 2018
© Author(s) 2018. CC BY 4.0 License.

hydrologists (Sampson and Gochis, 2018). Among the remaining eight sites, four have discontinuous or missing data over the calibration period. Therefore, we calibrated WRF-Hydro using four USGS sites (referred to as Station 1, Station 2, Station 3, and Station 4 hereafter), as shown in Fig. 1 with their site number. We then transfer the calibrated parameters to other sub-basins in the study area to assess the transferability of the calibrated parameters. Although there are many parameters, including spatially distributed parameters and constant parameters in the lookup tables, that affect the model performance, we only calibrate the parameters in lookup tables and do not consider the spatial variability of each parameter or their scaling factors. We acknowledge that there are studies that calibrate a single scaling factor of overland roughness coefficients (OVROUGHRTFAC) rather than the actual value of each land type in the lookup table (e.g., Kerandi et al., 2018). Although this approach reduces the number of calibrated parameters, it has less flexibility because changing one factor will change all the parameters that use the same proportion. In addition, a single scaling factor holds the same for the entire domain, which may work well for a small domain, but could be problematic for a large domain. Thus, we suggest the calibration of spatially distributed parameters requires more knowledge and understanding of the study area and deserves future studies. In this study, we calibrate the roughness coefficients for each land type rather than calibrating a single scaling factor.

For most calibration exercises we document here, the retention depth factor (RETDEPRTFAC) is fixed at 0.001. This value is reasonable because the modelled discharge of our particular configuration (Sect. 2.2) using default parameters is much lower than observed discharge. Reducing this factor from 1 to 0.001 keeps less water in water ponds and more water on the surface so it can contribute to river discharge. First, we calibrate 48 parameters based on a 3-day simulation from April 9 to 12, 2013 (Table S1 in Supporting Information). We calibrate the Manning's roughness coefficients for both channels and land-use types, the deep drainage (SLOPE), infiltration-scaling parameter (REFKDT), and saturated soil lateral conductivity (REFDK). The Manning's roughness coefficients control the hydrograph shape and the timing of the peaks; the infiltration factor, saturated hydraulic conductivity, and deep drainage control the total water volume. Second, based on the knowledge we learn from the 3-day calibration (see details in Sect. 4.1), we redefine the number of parameters to calibrate and the range of many parameters according to the literature (Soong et al., 2012) to maintain their physical meanings (Table 1). We

Geosci. Model Dev. Discuss., https://doi.org/10.5194/gmd-2018-253
Manuscript under review for journal Geosci. Model Dev.
Discussion started: 29 November 2018
© Author(s) 2018. CC BY 4.0 License.

also extend our calibration period to 7 days to include a heavy precipitation period. Although a period of 7 days is still very short compared to the traditional calibration period of at least 1 year, we find it provides more appropriate parameter estimation—as well as better results of simulated hydrograph shape and the total water volume—than does the 3-day calibration.

3.4 Statistics

This study employs three statistical criteria: Nash–Sutcliffe efficiency (NSE; Nash and Sutcliffe, 1970; Moriasi et al., 2007), root-mean-square error (RMSE), and Pearson correlation coefficient (PCC). RMSE and PCC evaluate model performance in terms of bias and temporal variation. NSE quantitatively describes the accuracy of modelled discharge compared to the mean of observed data. Equation (1) calculates the NSE with defined variables:

$$NSE = 1 - \frac{\sum_{t=0}^{n}\left(Y_t^{obs} - Y_t^{sim}\right)^2}{\sum_{t=0}^{n}\left(Y_t^{obs} - Y_{mean}^{sim}\right)^2}, \quad (1)$$

where Y_t^{obs} is the *t*th observed value from USGS sites for river discharge , $Y_t^{sim}$is the *t*th simulated value from the WRF-Hydro output, Y_{mean}^{obs} is the temporal average of USGS observed discharge, and *n* is the total number of observation time points. An efficiency of 1 (NSE = 1) corresponds to a perfect match between modeled discharge and observed data. An efficiency of 0 (NSE = 0) indicates that the model predictions are as accurate as the mean of the observed data. An efficiency below zero (NSE < 0) occurs when the model is worse than the observed mean. Essentially, the closer the NSE is to 1, the more accurate the model is.

4 Results

4.1 Three-day calibration and validation

Figure 2 shows the results of the 3-day modeled discharge (in cubic meters) using default and calibrated parameters, as well as observed discharge from April 9 to 12. After the fifth iteration, the difference in calibrated results between different iterations is relatively small, and PEST performed 12 iterations before finding the optimum parameters. Here we only show results generated by default parameters and by parameters calibrated from the 1st, 5th, and 12th iterations. Over Stations 2, 3, and 4, which sit on rivers with relatively large water volumes, the discharge modeled by the default parameters is much lower than discharge seen in observations. PEST

Geosci. Model Dev. Discuss., https://doi.org/10.5194/gmd-2018-253
Manuscript under review for journal Geosci. Model Dev.
Discussion started: 29 November 2018
© Author(s) 2018. CC BY 4.0 License.

detects this underestimation. It immediately adjusts the parameters and increases the modeled discharge during the first iteration. After adjusting the parameters for several iterations, the modeled discharge gets much closer to the observations compared to the modeled results that used the default parameters. Table 2 shows the statistics of model performance using default and calibrated parameters for all four stations during the calibration and validation period. Compared to the discharge that was modeled using the default WRF-Hydro parameters, overall, the calibrated modeled discharge matches observations better, especially at the three stations with large volumes of water. Note that this 3-day period only experienced a light rain over the study area. The streamflow in the rivers is, therefore, mostly from groundwater and overland flow from upstream or from previous precipitation events. The contribution of overland flow is small for this period because the amount of precipitation was also small, so the main contributor to river discharge in the real situation was from the groundwater. However, in this study WRF-Hydro uses a direct pass-through groundwater model, which does not account for slow discharge and long-term storage of the baseflow. Therefore, groundwater does not contribute much discharge to the channels. This situation causes the model to greatly underestimate discharge, so the calibration adjusts critical parameters aggressively to increase the streamflow to match the observations. When we apply these calibrated parameters to the following days, the calibrated discharge is much higher than the observed discharge during the heavy precipitation period, as shown by Fig. 3 and the RMSEs for the validation period in Table 2. However, after the heavy precipitation event, the modeled discharge decreases much faster than in the observed situation (Fig. 3). This again might be due to the direct pass-through groundwater model we adopt in this study, which uses an output-equals-input relationship between soil drainage and the discharge into river channels. This model does not allow long-term storage of baseflow in each conceptual bucket, and thereby not be able to fully represent the contribution of groundwater to streamflow.

From this 3-day calibration experiment, we learn that the WRF-Hydro output is not sensitive to several parameters we calibrated in this particular study. For example, Manning's roughness coefficients for several land types barely change during the calibration because these land types (e.g., tundra, snow/ice) are not present in the study period and area. We also learn that even though the calibrated WRF-Hydro parameters can generate discharge results that closely resemble observations, the physical meaning of several parameters are not appropriate due to the wide range

Geosci. Model Dev. Discuss., https://doi.org/10.5194/gmd-2018-253
Manuscript under review for journal Geosci. Model Dev.
Discussion started: 29 November 2018
© Author(s) 2018. CC BY 4.0 License.

of those parameters that we set in the PEST control file. For example, as shown in Table S1, the Manning's roughness coefficient for stream order 1 (0.199) is calibrated smaller than that for stream order 2 (0.218); the overland roughness coefficients for evergreen needleleaf forest (0.043) and mixed forest (0.023) are calibrated smaller than cropland/woodland (0.046). Neither of these is true in the real world.

4.2 Seven-day calibration and validation

Based on the knowledge we gained from the 3-day calibration, we adjust the range of critical parameters in the PEST control file. For example, we set the Manning's roughness coefficient larger for stream order 1 than for stream order 2. We also adjust the parameter range of the overland roughness coefficient for multiple land covers, such as forests. With the adjusted range of parameters, we perform 7-day calibration from 00:00 UTC on April 9, 2013, to 00:00 UTC on April 16, 2013, when there is an increased streamflow that the simulation does not capture using 3-day calibrated parameters. The entire calibration takes 12 iterations. Figure 4 shows the results of modeled discharge (in cubic meters) using default and calibrated parameters (from the first, fifth, and 12th iterations), as well as observed discharge from April 9 to 16. Over Stations 2, 3, and 4, the modeled discharge using the default parameter underestimates the streamflow by more than 100%. PEST detects this underestimation and starts adjusting parameters to increase the discharge to match the observations. Compared to the modeled discharge using default parameters during the validation period, as shown in Table 3, the RMSE decreased from 624.9 (Station 1), 5162.9 (Station 2), 4990.0 (Station 3), and 5098.3 m^3/sec (Station 4) to 283.1, 637.9, 666.8, and 1202.8 m^3/sec, respectively. The correlation coefficient between observed and modeled discharge increased from 0.71, 0.90, 0.87, and 0.82 to 0.97, 0.99, 0.96, and 0.86. Note that, although the calibration helps three stations (Station 2, 3, and 4) with large water volumes to generate more reasonable results than the default parameters, the results for Station 1, which has a relatively small volume of water, is not always better than the discharge that is modeled using default parameters (Tables 2 and 3). This might be because we use the same absolute weight for all the stations when we perform the calibration. Using a higher weight for Station 1 may help improve this situation and generate better results for this station.

Geosci. Model Dev. Discuss., https://doi.org/10.5194/gmd-2018-253
Manuscript under review for journal Geosci. Model Dev.
Discussion started: 29 November 2018
© Author(s) 2018. CC BY 4.0 License.

Although a period of 7 days is still very short for calibration compared to traditional calibration period of at least 1 year, we find that the 7-day period provides better and more appropriate parameter estimation than does the 3-day calibration, and it does a better job of capturing the hydrograph shape and the total water volume. Comparing the validation statistics between Tables 2 and 3 as well as Figs. 3 and 5, we find the 7-day calibrated parameters generate better results than do the 3-day calibrated parameters for both water volume and the hydrograph shape over the validation period. Compared to the discharge modeled using 3-day calibrated optimum parameters, there is a 17–33% increase in the simulated streamflow (1,400–2,800 m^3/sec) calculated over Station 2, 3, and 4 using the 7-day calibrated parameters from April 12 to 16. The RMSE is 3,400–3,600 m^3/sec when calculated using the 3-day calibration, but this decreases to 600–1,200 m^3/sec when calculated using the 7-day calibration. The correlation coefficient between observed and modeled discharge using the 7-day calibration is 0.8–0.99, but that using the 3-day calibration is only 0.7–0.8. However, there is still a problem with the temporal variability of the modeled discharge, especially over the rivers with large discharge. When there is precipitation, the discharge immediately increases and is higher than the observed discharge. After the precipitation period, when the observed discharge still stays high, the modeled discharge decreases sooner and thus is smaller than the observed discharge. This might be the direct pass-through approach simplified groundwater flow, and does not represent the interaction between stream flow and groundwater properly in this case study.

4.3 Evaluation of spatial transferability of the modeling system

In this section, we apply the calibrated parameters for the four stations (black circles) in Fig. 1 to other 13 stations in the study area. As mentioned before, because of inaccuracies in the spatial location of station data and digital elevation models, and because of small errors introduced when projecting geospatial data from one coordinate system to another using the ArcGIS tool, only four stations are mapped on the river systems (crosses in Fig. 1); others are slightly shifted out of their closest grid cell. One of these four sites (Station 5) is located on a relatively small river, and others are located on larger rivers. The following analyses assess the transferability of the calibrated parameters from particular sites to other sites that are in the study area but not calibrated. The assessment compares the observed discharge with the closest grid cells from the discharge output of WRF-Hydro. Figure 6 shows the observed and modeled discharge using default and calibrated

Geosci. Model Dev. Discuss., https://doi.org/10.5194/gmd-2018-253
Manuscript under review for journal Geosci. Model Dev.
Discussion started: 29 November 2018
© Author(s) 2018. CC BY 4.0 License.

parameters. Overall, WRF-Hydro's default parameters underestimate the discharge. WRF-Hydro also generates an earlier discharge peak compared to observations over the four stations (Stations 5, 6, 7, and 8) in this particular study. The calibrated model results increase the discharge and generate a hydrograph shape that is closer to the observations than the default model results do. The absolute error of simulated discharge decreases by 12.8%, 22.8%, 46.8%, and 49.9%, respectively, over Stations 5 through 8, compared to the default simulated discharge. However, because we did not specifically calibrate these stations based on observations, there are still differences between the calibrated results and observations.

5 Discussion and summary

5.1 Scale-up capabilities

The ability to scale up calibration of WRF-Hydro using parallel PEST on HPCs is determined by two factors: the scale-up capability of WRF-Hydro, and the scale-up capability of PEST. In the course of calibrating WRF-Hydro, PEST must run the WRF-Hydro model many times. PEST makes some model runs to calculate Jacobian matrix (Doherty, 2016). These model runs are independent between slaves. Each slave run the model using temporarily incremented parameters that are defined in the template and control files. These model runs can be easily parallelized. However, PEST also need to make some other model runs to test parameter upgrades. These runs are calculated based on different Marquardt lambdas. The search for a Marquardt lambda that achieves the best set of parameters is a serial procedure — what lambda to use next depends on the outcome of the model run conducted using the previously chosen lambda. This in fact is the major bottleneck of parallelization of the PEST code. Although serial testing of Marquardt lambdas may quickly find the optimal Marquardt lambda in the first or second series of model runs, it is an inefficient use of computing resources because other processors are idle while only one process is searching the lambdas. This is especially true when the model domain is large and requires extensive computing resources.

This study employs "partial parallelization" for the lambda-testing procedure (Doherty, 2016), so all the processors can be used to calculate parameter upgrades based on a series of lambda values that are related to each other by a factor of RLAMFAC set in the PEST control file. This partial

Geosci. Model Dev. Discuss., https://doi.org/10.5194/gmd-2018-253
Manuscript under review for journal Geosci. Model Dev.
Discussion started: 29 November 2018
© Author(s) 2018. CC BY 4.0 License.

parallelization makes the scale up challenging when more processors are in use, because generating many Marquardt lambdas does not always guarantee that the best Marquardt lambdas were the ones generated. As a result, the calibration process may converge more slowly when using more slaves than it does when using less slaves. We tested different numbers of slaves (35, 50, 70, and 105) for the 32-parameter calibration experiment. In total, each of these tests uses 71, 101, 141, and 211 nodes; two nodes for each slave run WRF-Hydro, and one node runs PEST master to coordinate jobs and communicate with the slaves. The results shown in Figs. 2–6 and Tables 2–3 are from a calibration using 35 slaves; PEST conducted 12 iterations before finding the optimum parameters. We find that using different numbers of slaves generates slightly different parameter values and involves different numbers of iterations. For example, using 70 slaves only takes eight iterations and 41% of the wall-clock time 35 slaves used to find the optimum parameters. The calibrated parameters are slightly different from those generated by 35 slaves (Table 1, last column), and they generate slightly better results than does the 35-slave test compared to observed discharge. We finish the 12 iterations using 35 slaves (71 nodes) within 73 hours, and the eight iterations using 70 slaves (141 nodes) within 30 hours. More than 800 model runs were conducted for entire calibration process including calculating the Jacobian Matrix as well as testing the parameter upgrades. In fact if more nodes were used by each slave for the calculation, the wall-clock time can be further reduced. If these calibration were conducted sequentially on personal computers, the same calibration process would have taken 60–80 days for a 7-day calibration.

Our study finds that, depending on the number of parameters being calibrated (e.g., 32 parameters in this particular study), using 32 to 64 slaves shows fairly good scale-up capability; most of the time consumed by PEST is for running WRF-Hydro, and the number of slaves can be used to carry out model runs to generate the Jacobian matrix. However, using 105 slaves (211 nodes) does not result in fewer iterations or a shorter wall-clock time than using 70 slaves. In fact, using more than 64 slaves may not be necessary because generating many Marquardt lambdas does not always guarantee generating the best Marquardt lambdas. In addition, at least for the calibrations conducted in this study, in each iteration, PEST runs the model either 32 or 64 times to calculate the Jacobin matrix. Therefore, having more than 64 slaves would most likely render some slaves idle and is not an efficient use of computing resources.

Geosci. Model Dev. Discuss., https://doi.org/10.5194/gmd-2018-253
Manuscript under review for journal Geosci. Model Dev.
Discussion started: 29 November 2018
© Author(s) 2018. CC BY 4.0 License.

5.2 Summary

WRF-Hydro is a new, and perhaps the first practical, computer code that can run on HPCs and can model the entire hydrological cycle using physics-based sub-models and very high-resolution input datasets (e.g., radar). The hydrological community has desired this capability for decades, although it requires intensive computing resources. Thus, the calibration of this model would ideally be conducted on HPCs in parallel as well, especially when the model covers a large domain rather than the basin scale. This study ports an independent model calibration tool, parallel PEST, to HPC clusters and links it to WRF-Hydro to help WRF-Hydro users calibrate the model within a much shorter wall-clock period. This tool's uniqueness lies in its flexibility and robustness to calibration any parameters in WRF-Hydro. It is also unique in its use of two levels of parallelization across many slaves running PEST, with each slave running a simulation of WRF-Hydro. The calibration tool presented in this study also applies to any other hydrological models and similar earth system models that use parameterization to model physics. We present the optimum parameters identified from the calibration of this particular study case and area, but the calibrated parameters can be significantly different if one uses different physics, such as exponential storage-discharge function for a groundwater model, or reach-based channel routing.

We apply the HPC-enabled parallel PEST to WRF-Hydro to investigated a major flood event that occurred over the Midwestern United States in April 2013. Our precipitation inputs were derived from a radar, gauge, and satellite rainfall product named Stage IV. The calibrated parameters include Manning's roughness coefficients for both channels and land-use types, deep drainage, the infiltration scaling parameter, and saturated soil lateral conductivity. We evaluated the performance of WRF-Hydro in hydrograph features such as volume and timing of flood events. We also assessed the spatial transferability of the calibrated parameters in the study area.

The following are the primary findings of this study:

1. For this particular study, the HPC-enabled PEST calibration tool can speed up WRF-Hydro calibration by a factor of 30, compared to a serial calibration procedure.

© Author(s) 2018. CC BY 4.0 License.

2. Calibrated WRF-Hydro improves the modeled hydrographs compared to the default model results. The RMSE of discharge over the three large stations are reduced by 76–86% with calibration for the validation period.
3. Although the calibration period in this study is relatively short, we found that the longer the calibration period is, the better the model results are when compared to observations. It is difficult to precisely define what length of data is sufficient to identify model parameters so that they can also be used for other periods, because different models have different levels of complexity and different catchments have different information content in each year of hydrological record. Because of the heavy computation load for the calibration of WRF-Hydro, it would be challenging to calibrate yearlong time series.
4. Although there are inaccuracies when mapping the USGS stations onto the river systems, we found the WRF-Hydro calibrated parameters are helpful for nearby locations. The absolute bias over the four assessed stations decreased by 12–50% as a result of using the calibrated parameters, compared to using the default parameters for their simulations. The mapping issue are often random, or non-systematic; there is no generalizable way to automate the correction procedure with a high degree of fidelity. Manual manipulation or specification of the data is often required (Sampson and Gochis 2018).
5. Using different groundwater models can generate very different results and will require a completely different set of parameters for WRF-Hydro to model the observed discharge. Our preliminary testing shows that, using exponential storage-discharge function with the default parameters provided by WRF-Hydro, the modeled discharge was larger than observations. Thus, the calibration will need to adjust the parameters to reduce the discharge.

Data and Code availability. The observed river discharge is downloaded from the USGS Surface-Water Data website, available at https://waterdata.usgs.gov/nwis/sw. The Stage IV precipitation data were downloaded from https://data.eol.ucar.edu/dataset/21.093. PEST was downloaded from http://www.pesthomepage.org/Downloads.php. We use the Unix PEST version 13.6. The scripts and files that are developed in this study and required by PEST for calibrating WRF-Hydro are available at https://www.zenodo.org/record/1490230#.W_XI6TFRdhE. DOI: 10.5281/zenodo.1490230.

© Author(s) 2018. CC BY 4.0 License.

Author contributions. JW proposed the project and developed the study case in WRF and WRF-Hydro. CW developed the scripts/code to port the parallel PEST to DOE supercomputers and adapt it to work with WRF-Hydro. AO operated the ArcGIS tool to delineate the high resolution grid cells to include stream channel network, open water and groundwater/baseflow basins. RK provide high-level guidance and insight for the entire project. All authors commented on this manuscript.

Competing interests. The authors declare that they have no conflict of interest

Acknowledgements. This work is supported under a Laboratory Directed Research and Development (LDRD) Program at Argonne National Laboratory, through U.S. Department of Energy (DOE) contract DE-AC02-06CH11357. Computational resources are provided by the DOE-supported National Energy Research Scientific Computing Center, Argonne National Laboratory Computing Resource Center, and Argonne Leadership Computing Facility. Our special thanks to PEST developer John Doherty and the entire WRF-Hydro team, especially Kevin Sampson, for his guidance on the ArcGIS tool.

References

Arnault, J., Wagner, S., Rummler, T., Fersch, B., Bliefernicht, J., Andresen, S., and Kunstmann, H.: Role of runoff–infiltration partitioning and resolved overland flow on land–atmosphere feedbacks: A case study with the WRF-Hydro coupled modeling system for West Africa, J. Hydrometeorol., 17, 1489–1516, 2016.

Campos, E. and Wang, J.: Numerical simulation and analysis of the April 2013 Chicago Floods, J. Hydrol., 531, 454–474, 2015.

Chen, F. and Dudhia, J.: Coupling an advanced land surface-hydrology model with the Penn State-NCAR MM5 modeling system. Part I: Model implementation and sensitivity, Mon. Weather Rev., 129, 569–585, 2001.

© Author(s) 2018. CC BY 4.0 License.

Doherty, J.: PEST: Model Independent Parameter Estimation, User Manual, 6th ed., Watermark Numerical Computing, Brisbane, Queensland, Australia, 2016.

Getirana, A. C. V.: Integrating spatial altimetry data into the automatic calibration of hydrological models, J. Hydrol., 387 (3-4), 244–255, doi: 10.1016/j.jhydrol.2010.04.013, 2010.

Gochis, D. J. and Chen, F.: Hydrological enhancements to the community Noah land surface model, NCAR Technical Note NCAR/TN-454+STR, doi: 10.5065/D60P0X00, 2003.

Gochis, D.J., M. Barlage, A. Dugger, K. FitzGerald, L. Karsten, M. McAllister, J. McCreight, J. Mills, A. RafieeiNasab, L. Read, K. Sampson, D. Yates, W. Yu, (2018). The WRF-Hydro modeling system technical description, (Version 5.0). NCAR Technical Note. 107 pages. Available online at: https://ral.ucar.edu/sites/default/files/public/WRFHydroV5TechnicalDescription.pdf.

Kerandi, N., Arnault, J., Laux, P., Wagner, S., Kitheka, J., and Kunstmann, H.: Joint atmospheric-terrestrial water balances for East Africa: A WRF-Hydro case study for the upper Tana River basin, Theor. Appl. Climatol., 131, 1337–1355, doi: 10.1007/s00704-017-2050-8, 2018.

Levenberg, K.: A method for the solution of certain non-linear problems in least squares, Q. Appl. Math., 2(2), 164–168, 1944.

Lin, Y. and Mitchell, K. E.: The NCEP stage II/IV hourly precipitation analyses: Development and applications, Preprints, 19th Conf. on Hydrology, San Diego, CA, Amer. Meteor. Soc., 1.2., 2005.

Madsen, H.: Automatic calibration of a conceptual rainfall–runoff model using multiple objectives, J. Hydrol., 235, 276–288, 2000.

Marquardt, D. W.: An algorithm for least-squares estimation of non-linear parameters, J. Soc. Indust. Appl. Math., 11(2), 431–441, 1963.

© Author(s) 2018. CC BY 4.0 License.

Moriasi, D. N., Arnold, J. G., Van Liew, M. W., Bingner, R. L., Harmel, R. D., and Veith, T. L.: Model evaluation guidelines for systematic quantification of accuracy in watershed simulations, Transactions of the ASABE, 50 (3), 885–900, 2007.

Nash, J. E. and Sutcliffe, J. V.: River flow forecasting through conceptual models part I — A discussion of principles, J. Hydrol., 10(3), 282–290, doi: 10.1016/0022-1694(70)90255-6, 1970.

Niu, G.-Y., Yang, Z.-L., Mitchell, K. E., Chen, F., Ek, M. B., Barlage, M., Kumar, A., Manning, K., Niyogi, D., Rosero, E., Tewari, M., and Xia, Y.: The community Noah land surface model with multiparameterization options (Noah-MP): 1. Model description and evaluation with local-scale measurements, J. Geophys. Res., 116, D12109, doi: 10.1029/2010JD015139, 2011.

NWS (National Weather Service): Record River Flooding of April 2013, https://www.weather.gov/ilx/apr2013flooding, 2013.

Papathanasiou, C., Makropoulos, C., and Mimikou, M.: Hydrological modelling for flood forecasting: Calibrating the post-fire initial conditions, J. Hydrol., 529, 1838–1850, doi: 10.1016/j.jhydrol.2015.07.038, 2015.

Prat, O. P. and Nelson, B. R.: Evaluation of precipitation estimates over CONUS derived from satellite, radar, and rain gauge data sets at daily to annual scales (2002-2012), Hydrol. Earth Syst. Sci., 19, 2037–2056, doi: 10.5194/hess-19-2037-2015, 2015.

Sampson, K. and Gochis, D.: WRF Hydro GIS Pre-Processing Tools, Version 5.0 Documentation, 2018.

Sapiano, M. R. P. and Arkin, P.A.: An intercomparison and validation of high-resolution satellite precipitation estimates with 3-hourly gauge data, J. Hydrometeor., 10, 149–166, doi: 10.1175/2008JHM1052.1, 2009.

© Author(s) 2018. CC BY 4.0 License.

Senatore, A., Mendicino, G., Gochis, D. J., Yu, W., Yates, D. N., and Kunstmann, H.: Fully coupled atmosphere-hydrology simulations for the central Mediterranean: Impact of enhanced hydrological parameterization for short and long time scales, J. Adv. Model. Earth Syst., 7(4), 1693–1715, doi: 10.1002/2015MS000510, 2015.

Soong, D. T., Prater, C. D., Halfar, T. M., and Wobig, L. A.: Manning's roughness coefficients for Illinois streams, U.S. Geological Survey Data Series 668, 2012.

Xia, Y., Mitchell, K., Ek, M., Sheffield, J., Cosgrove, B., Wood, E., Luo, L., Alonge, C., Wei, H., Meng, J., Livneh, B., Lettenmaier, D., Koren, V., Duan, Q., Mo, K., Fan, Y., and Mocko, D.: Continental-scale water and energy flux analysis and validation for the North American Land Data Assimilation System project phase 2 (NLDAS-2). 1: Intercomparison and application of model products, J. Geophys. Res., 117, D03109, doi: 10.1029/2011JD016048, 2012a.

Xia, Y., Mitchell, K., Ek, M., Cosgrove, B., Sheffield, J., Luo, L., Alonge, C., Wei, H., Meng, J., Livneh, B., Duan, Q., and Lohmann, D.: Continental-scale water and energy flux analysis and validation for the North American Land Data Assimilation System project phase 2 (NLDAS-2). 2. Validation of model-simulated streamflow, J. Geophys. Res., 117, D03110, doi: 10.1029/2011JD016051, 2012b.

Yucel, I., Onen, A. Yilmaz, K. K., and Gochis, D. J.: Calibration and evaluation of a flood forecasting system: Utility of numerical weather prediction model, data assimilation and satellite-based rainfall, J. Hydrol., 523, 49–66, 2015.

Zanon, F., Borga, M., Zoccatelli, D., Marchi, L., Gaume, E., Bonnifait, L., Delrieu, G.: Hydrological analysis of a flash flood across a climatic and geologic gradient: The September 18, 2007 event in Western Slovenia, J. Hydrol., 394, 182–197, doi: 10.1016/j.jhydrol.2010.08.020, 2010.

Figure captions:

Geosci. Model Dev. Discuss., https://doi.org/10.5194/gmd-2018-253
Manuscript under review for journal Geosci. Model Dev.
Discussion started: 29 November 2018
© Author(s) 2018. CC BY 4.0 License.

Geoscientific Model Development Discussions

Figure 1: Eight USGS sites over the study area. The four circles are sites that are used for calibrations; the four crosses are sites that are used for transferability assessment. USGS site numbers corresponding to the site index used in this study are listed on the top left corner of the map.

Figure 2: Observed and modeled discharge (m^3/sec) using default and calibrated parameters during a 3-day calibration period (April 9–12, 2013) over the four stations indicated by the black circles in Fig. 1.

Figure 3: Observed and modeled discharge (m^3/sec) using optimum parameters identified from a 3-day calibration during a validation period (April 13–24, 2013) over the four stations indicated by black circles in Fig. 1.

Figure 4: Same as Fig. 2, but during a 7-day calibration period (April 9–15, 2013).

Figure 5: Same as Fig. 3, but the modeled discharge uses 7-day calibrated parameters over a validation period from April 17 to 24, 2013.

Figure 6: Observed and modeled discharge (m^3/sec) using default and the optimum parameters identified by a 7-day calibration over four stations that are in the study area (indicated by crosses in Fig. 1).

Geosci. Model Dev. Discuss., https://doi.org/10.5194/gmd-2018-253
Manuscript under review for journal Geosci. Model Dev.
Discussion started: 29 November 2018
© Author(s) 2018. CC BY 4.0 License.

Geoscientific Model Development Discussions
Open Access
EGU

Table 1: 7-day calibrated parameters and the optimum parameter found by the calibration.

Calibrated parameters	Default	Lower bound	Upper bound	Optimum parameters 35 slaves (12[a])	Optimum parameters 70 slaves (8[a])
mannn1	0.55	0.35	0.6	0.440658	0.469277
mannn2	0.35	0.15	0.35	0.35	0.209592
mannn3	0.15	0.08	0.15	8.00E-02	8.00E-02
mannn4	0.1	0.05	0.15	0.15	0.15
mannn5	7.00E-02	0.02	0.1	6.13E-02	8.59E-02
mannn6	5.00E-02	0.015	0.1	1.50E-02	1.50E-02
mannn7	4.00E-02	0.01	0.08	1.41E-02	1.36E-02
mannn8	3.00E-02	0.005	0.06	5.00E-03	1.12E-02
mannn9	2.00E-02	0.003	0.05	3.00E-03	5.00E-03
mannn10	1.00E-02	0.0001	0.03	4.09E-04	1.00E-04
xslope1	0.1	1.00E-04	1	0.64603	0.663051
refdk	2.00E-06	1.00E-08	1.00E-05	9.85E-08	1.83E-07
refkdt	1	0.01	5	4.98912	1.49769
ovn1	2.50E-02	0.005	0.06	2.12E-02	5.00E-03
ovn2	3.50E-02	0.015	0.06	6.00E-02	6.00E-02
ovn3	3.50E-02	0.015	0.06	5.45E-02	6.00E-02
ovn4	5.50E-02	0.015	0.1	5.50E-02	5.50E-02
ovn5	3.50E-02	0.015	0.06	6.00E-02	6.00E-02
ovn6	6.80E-02	0.035	0.25	3.50E-02	0.144637
ovn7	5.50E-02	0.015	0.25	1.50E-02	1.75E-02
ovn8	5.50E-02	0.015	0.25	5.50E-02	5.50E-02
ovn9	5.50E-02	0.015	0.25	5.50E-02	5.50E-02
ovn10	5.50E-02	0.015	0.3	1.50E-02	1.50E-02
ovn11	0.2	0.1	0.3	0.27072	0.3
ovn12	0.2	0.1	0.3	0.1	0.20025
ovn13	0.2	0.1	0.3	0.1	0.20025
ovn14	0.2	0.1	0.3	0.291836	0.1
ovn15	0.2	0.1	0.3	0.1	0.1
ovn16	5.00E-03	0.001	0.01	1.00E-03	1.00E-03
ovn17	7.00E-02	0.005	0.1	7.27E-02	7.01E-02
ovn18	7.00E-02	0.005	0.1	7.27E-02	7.01E-02
ovn19	3.50E-02	0.015	0.06	4.04E-02	3.52E-02

[a] Number of iterations during the calibration before finding the optimum parameter.

Geosci. Model Dev. Discuss., https://doi.org/10.5194/gmd-2018-253
Manuscript under review for journal Geosci. Model Dev.
Discussion started: 29 November 2018
© Author(s) 2018. CC BY 4.0 License.

Table 2: Statistics of model performance using optimum and default (in the parenthesis) parameters for Stations 1-4 during the calibration and validation period.[a]

Statistics	Station 1	Station 2	Station 3	Station 4
		Calibration		
NSE	0.14 (0.73)	**0.70 (-54.4)**	**0.49 (-157.3)**	**-3.7 (-1316.9)**
RMSE	123.6 (69.7)	**292.7 (3944.7)**	**227.2 (4001.1)**	**263.7 (4413.2)**
PCC	**0.97 (0.91)**	0.90 (0.92)	**0.94 (0.87)**	**0.83 (0.66)**
		Validation		
NSE	**0.83 (0.39)**	**-0.51 (-4.2)**	**-0.81 (-46.5)**	**-1.02 (-5.54)**
RMSE	**276.9 (528.3)**	**3452.1 (6410.9)**	**3416.8 (17503.4)**	**3694.5 (6655.6)**
PCC	**0.96 (0.8)**	**0.80 (0.76)**	**0.76 (0.21)**	0.72 (0.72)

[a] The calibration period is 3 days (April 9–12) and includes 48 parameters. The validation period is April 13–23. Bold typeface indicates the calibrated model results are closer to observations compared to the default model results. NSE and PCC are unitless; RMSE is in m^3/sec.

Geosci. Model Dev. Discuss., https://doi.org/10.5194/gmd-2018-253
Manuscript under review for journal Geosci. Model Dev.
Discussion started: 29 November 2018
© Author(s) 2018. CC BY 4.0 License.

Geoscientific Model Development Discussions

Table 3: Same as Table 2, but for 7-day calibration.[a]

Statistics	Station 1	Station 2	Station 3	Station 4
		Calibration		
NSE	-0.53 (-0.19)	**0.99 (-4.6)**	**0.98 (0.12)**	**0.92 (0.1)**
RMSE	217.3 (191.2)	**241 (5162.9)**	**273.6 (4990.9)**	**607.8 (5098.3)**
COR	**0.83 (0.64)**	**0.99 (0.90)**	**0.96 (0.87)**	**0.86 (0.82)**
		Validation		
NSE	**0.86 (0.30)**	**0.91 (-4.6)**	**0.9 (-4.1)**	**-0.69 (-4.6)**
RMSE	**283.1 (624.9)**	**637.9 (5162.9)**	**666.8 (4990.9)**	**1202.8 (5098.3)**
COR	**0.97 (0.71)**	**0.99 (0.90)**	**0.96 (0.87)**	**0.86 (0.82)**

[a] The calibration period is 7 days (April 9–12) and includes 48 parameters. The validation period is April 13–23. Bold typeface indicates the calibrated model results are closer to observations compared to the default model results. NSE and COR are unitless; RMSE is in m^3/sec.

Geosci. Model Dev. Discuss., https://doi.org/10.5194/gmd-2018-253
Manuscript under review for journal Geosci. Model Dev.
Discussion started: 29 November 2018
© Author(s) 2018. CC BY 4.0 License.

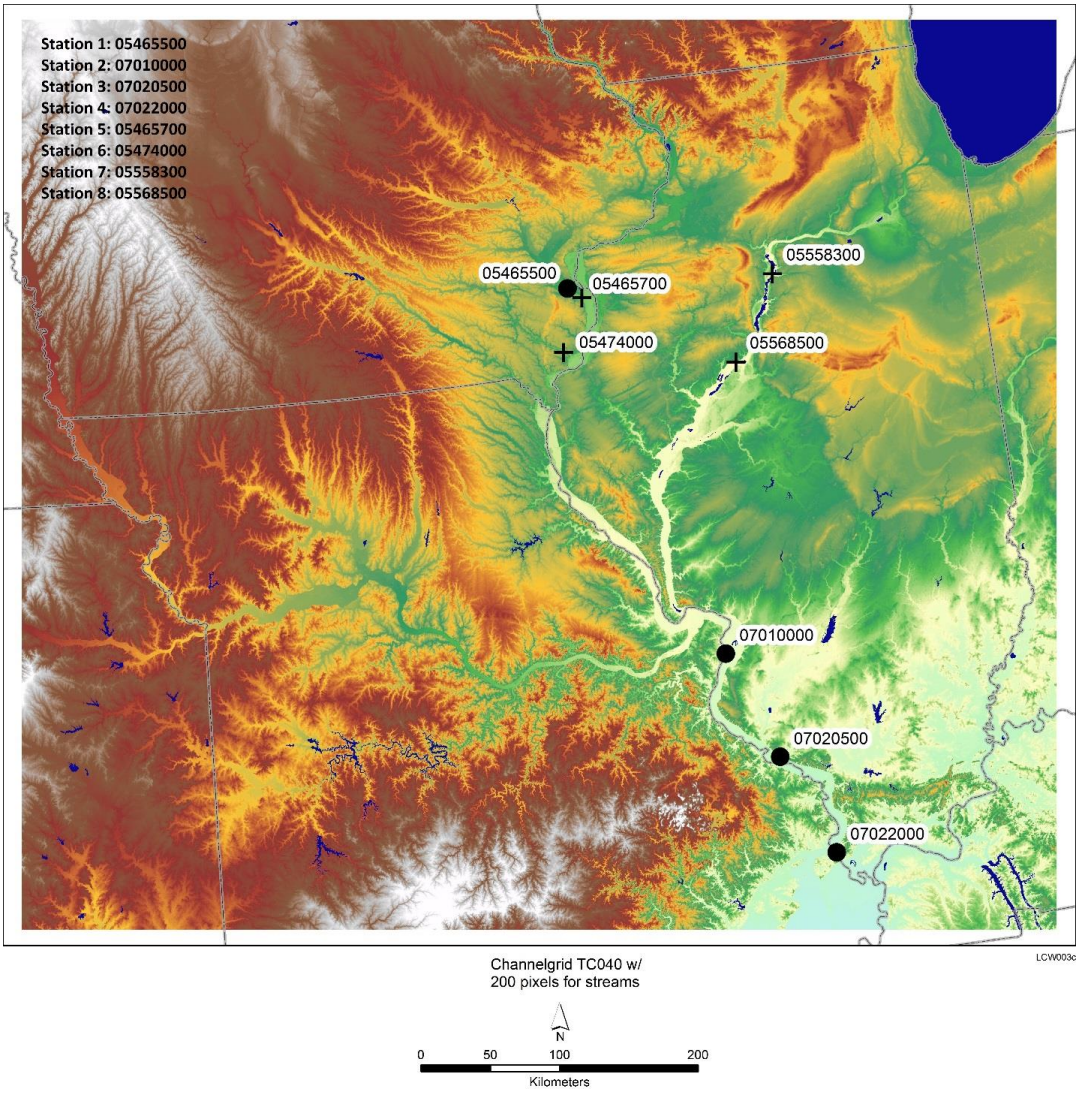

Figure 1: Eight USGS sites over the study area. The four circles are sites that are used for calibrations; the four crosses are sites that are used for transferability assessment. USGS site numbers corresponding to the site index used in this study are listed on the top left corner of the map.

Geosci. Model Dev. Discuss., https://doi.org/10.5194/gmd-2018-253
Manuscript under review for journal Geosci. Model Dev.
Discussion started: 29 November 2018
© Author(s) 2018. CC BY 4.0 License.

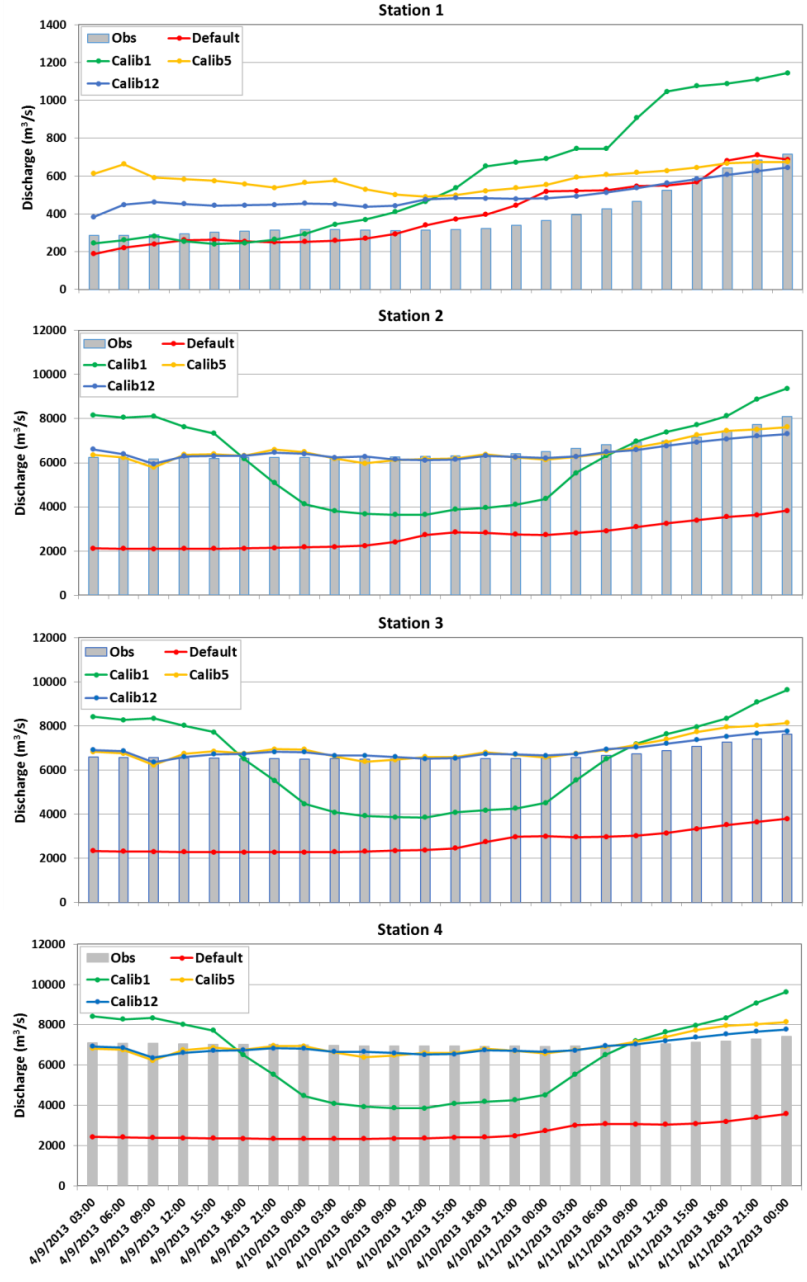

Figure 2: Observed and modeled discharge (m^3/sec) using default and calibrated parameters during a 3-day calibration period (April 9–12, 2013) over the four stations indicated by the black circles in Fig. 1.

Geosci. Model Dev. Discuss., https://doi.org/10.5194/gmd-2018-253
Manuscript under review for journal Geosci. Model Dev.
Discussion started: 29 November 2018
© Author(s) 2018. CC BY 4.0 License.

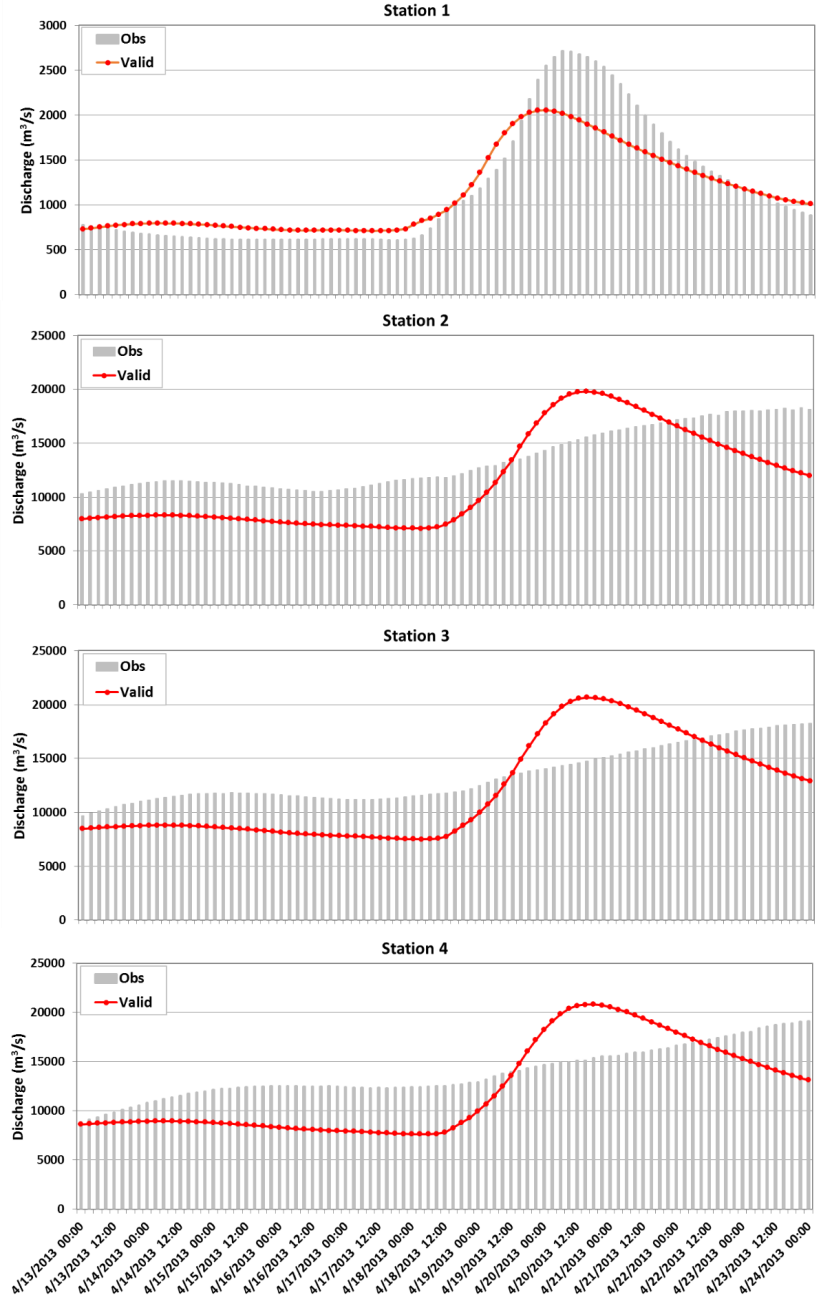

Figure 3: Observed and modeled discharge (m^3/sec) using optimum parameters identified from a 3-day calibration during a validation period (April 13–24, 2013) over the four stations indicated by black circles in Fig. 1.

Geosci. Model Dev. Discuss., https://doi.org/10.5194/gmd-2018-253
Manuscript under review for journal Geosci. Model Dev.
Discussion started: 29 November 2018
© Author(s) 2018. CC BY 4.0 License.

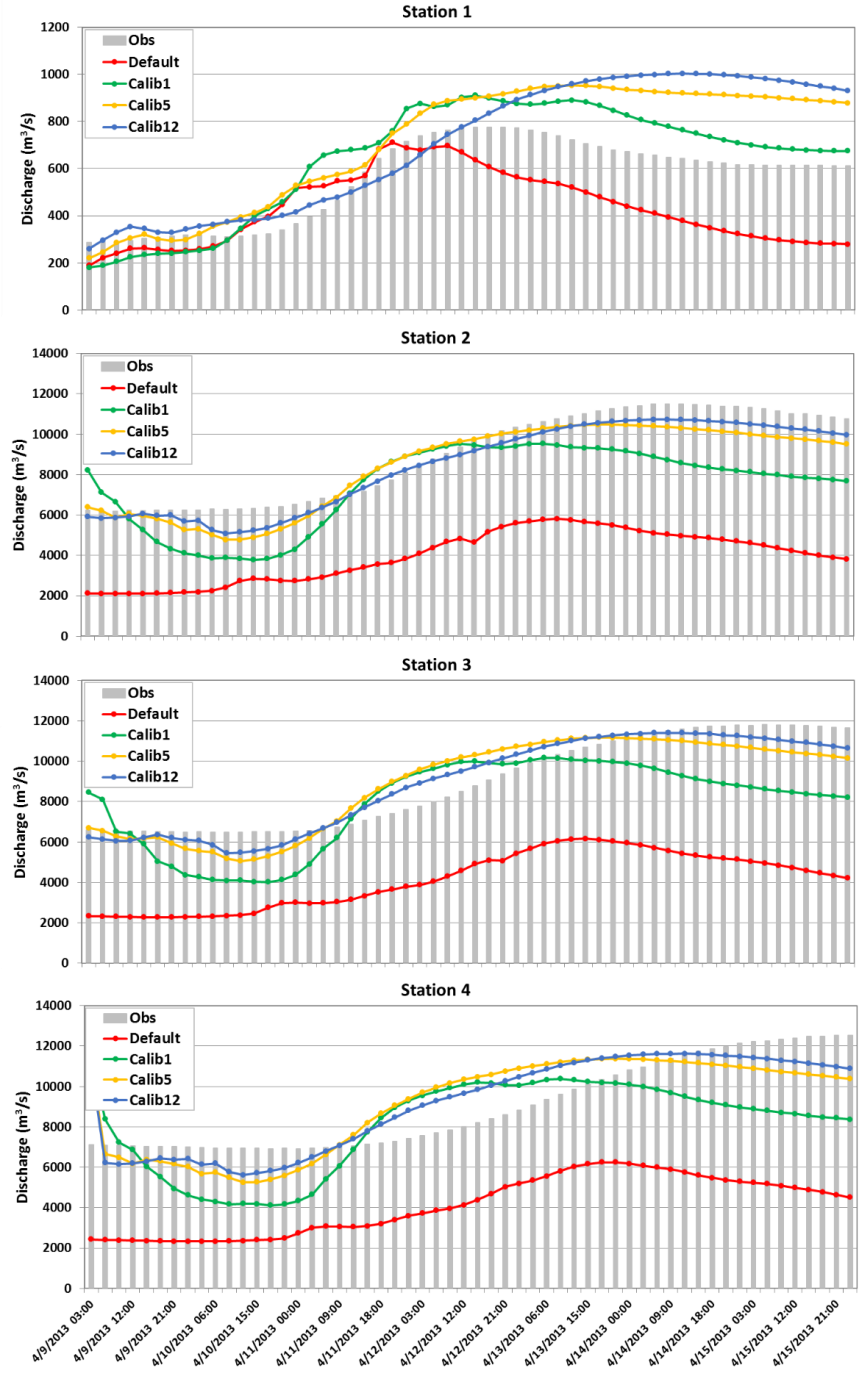

Figure 4: Same as Fig. 2, but during a 7-day calibration period (April 9–15, 2013).

Geosci. Model Dev. Discuss., https://doi.org/10.5194/gmd-2018-253
Manuscript under review for journal Geosci. Model Dev.
Discussion started: 29 November 2018
© Author(s) 2018. CC BY 4.0 License.

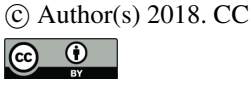

Geoscientific Model Development Discussions

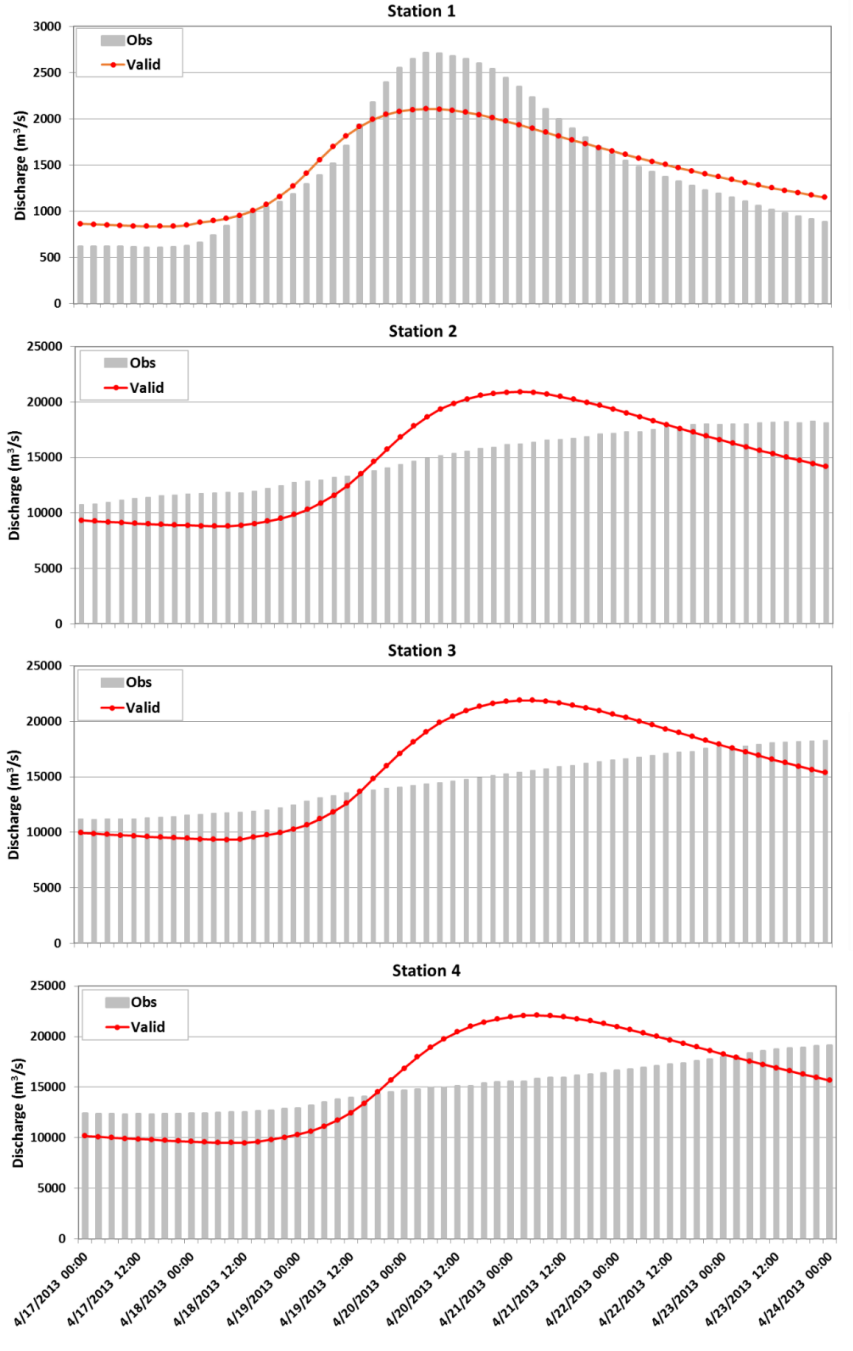

Figure 5: Same as Fig. 3, but the modeled discharge uses 7-day calibrated parameters over a validation period from April 17 to 24, 2013.

Geosci. Model Dev. Discuss., https://doi.org/10.5194/gmd-2018-253
Manuscript under review for journal Geosci. Model Dev.
Discussion started: 29 November 2018
© Author(s) 2018. CC BY 4.0 License.

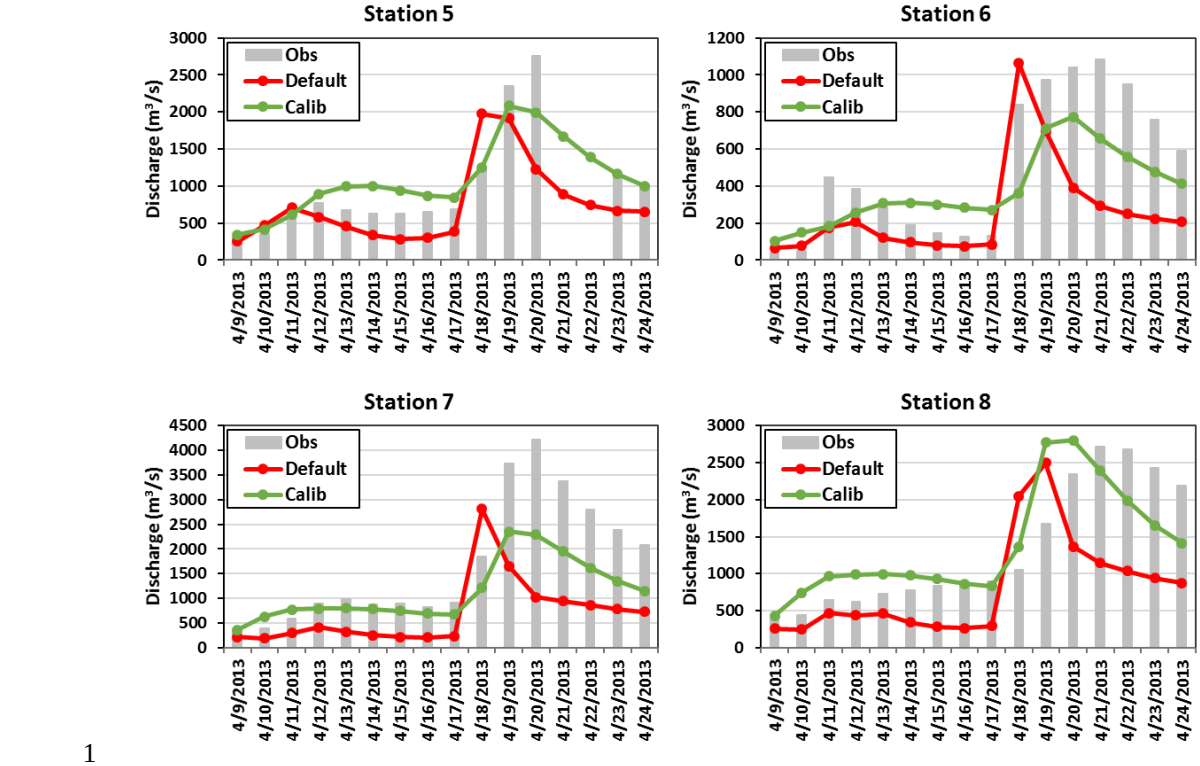

Figure 6: Observed and modeled discharge (m^3/sec) using default and the optimum parameters identified by a 7-day calibration over four stations that are in the study area (indicated by crosses in Fig. 1).